Ultrasensitive Label-Free Detection of PNA–DNA Hybridization by Reduced Graphene Oxide Field-Effect Transistor Biosensor

Bingjie Cai,[†] Shuting Wang,[†] Le Huang,[‡] Yong Ning,[†] Zhiyong Zhang,[‡,*] and Guo-Jun Zhang[†,*]

[†]School of Laboratory Medicine, Hubei University of Chinese Medicine, 1 Huangjia Lake West Road, Wuhan 430065, People's Republic of China, and [‡]Key Laboratory for the Physics and Chemistry of Nanodevices, Department of Electronics, Peking University, No. 5 Yiheyuan Road Haidian District, Beijing 100871, People's Republic of China

ABSTRACT A reduced graphene oxide (R-GO)-based field-effect transistor (FET) biosensor used for ultrasensitive label-free detection of DNA *via* peptide nucleic acid (PNA)–DNA hybridization is reported. In this work, R-GO was prepared by reduction of GO with hydrazine, and the FET biosensor was fabricated by drop-casting the R-GO suspension onto the sensor surface. PNA instead of DNA as the capture probe was employed, and DNA detection was performed through PNA–DNA hybridization by the R-GO FET biosensor. The detection limit as low as 100 fM was achieved, which is 1 order of magnitude lower than that of the previously reported graphene FET DNA biosensor based on DNA–DNA hybridization. Moreover, the R-GO FET biosensor was able to distinguish the complementary DNA from one-base mismatched DNA and noncomplementary DNA. Interestingly, the fabricated DNA biosensor was found to have a regeneration capability. The developed R-GO FET DNA biosensor shows ultrasensitivity and high specificity, indicating its potential applications in disease diagnostics as a point-of-care tool.

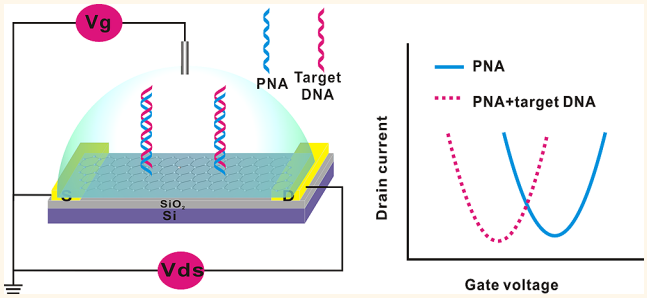

KEYWORDS: graphene · field-effect transistor biosensor · detection · peptide nucleic acid · DNA · hybridization

It is of great importance to develop ultrasensitive and high specific methods to detect DNA, for it can provide useful information for research of molecular biology,[1,2] diagnosis of genetic disease,[3,4] environment monitoring,[5,6] and so on. So far, there are many nanomaterial-based methods used for detecting DNA. For example, graphene oxide (GO)-based fluorescent sensors have been a platform for the detection of DNA,[7–9] electrochemical biosensors have widely been used for detecting DNA,[6,10,11] and field-effect transistor (FET) biosensors have also been developed to detect DNA.[12–14] Among them, the label-free FET biosensors have recently attracted much attention because they do not require fluorescent or electrochemical tags but attain high sensitivity and selectivity.[14,15]

During the past decades, nanomaterial-based FET biosensors, such as one-dimensional (1D) Si nanowire (SiNW) and carbon nanotube (CNT) devices, have attracted significant attention for label-free detection of chemical and biological species.[16–21] Graphene, a one-atom-thick 2D carbon material, has the potentials to exceed CNTs and SiNWs because of its high carrier mobility and ambipolar field effect,[14] large detection area, ease of functionalization,[22] and low intrinsic electrical noises.[23] As a result, the 2D graphene-based FET biosensor shows potential advantages over the 1D nanomaterial-based biosensors.

Recently, the highly sensitive and selective graphene FET biosensors have been developed in detecting biomolecules. For instance, Chen and co-workers[24] developed a rapid method for *Escherichia coli* bacteria detection by thermally reduced graphene oxide (TRGO) FET devices, in which the monolayer GO was produced by ultrasonic-assisted self-assembly. Kim *et al.*[25] detected a prostate cancer biomarker at femtomolar level through prostate-specific

* Address correspondence to zhanggj@hbtcm.edu.cn, zyzhang@pku.edu.cn.

Received for review December 10, 2013 and accepted February 14, 2014.

Published online February 14, 2014
10.1021/nn4063424

antigen monoclonal antibody (PSA mAb)-modified R-GO FET. Ohno *et al.*[26] used electrolyte-gated graphene FET for detecting protein adsorption at a picomolar level without any surface functionalization of the graphene. Li and co-workers[14,27] reported a liquid-gated FET biosensor based on CVD-grown graphene for label-free DNA detection, in which DNA was employed as the capture probe for detection of the target DNA with a low detection limit.

There are various methods to produce single- or few-layer graphene, such as mechanical exfoliation of graphite,[28,29] chemical vapor deposition (CVD),[30,31] reduction of graphene oxide (GO),[32,33] and so on. Low yield of mechanical exfoliation limits the large-scale use of this method. Meanwhile, high cost of CVD is also an obstacle in the bulk production of graphene sheets. Therefore, chemical reduction of GO, which is low-cost, simple, and efficient, appears to be a promising alternative. Meanwhile, PNA, a DNA mimic, whose negatively charged deoxyribose phosphate backbone is replaced with a neutral peptide backbone,[34,35] enables a high sensitivity because of its neutral character which eliminates electrostatic repulsion between the two hybridized strands and reduces the background.[36] What's more, the PNA probe has a great sequence-specific affinity and stability due to the proper distance between the nucleobases, the rigid amido bonds, the high flexibility of the aminoethyl linkers, and intramolecular hydrogen bonding.[37] We even developed the PNA-functionalized SiNW FET biosensor for DNA detection, in which PNA was immobilized on the oxide-etched SiNW surface.[12,36] However, the "top-down" fabrication process for such a nanowire-based FET biosensor was very tedious including more than 60 steps, leading to an expensive cost.

In this paper, we propose a new reduced graphene oxide (R-GO) FET biosensor for label-free detection of PNA–DNA hybridization with ultrasensitivity and high specificity. This is the first example of using the PNA-functionalized R-GO FET biosensor for DNA detection, whose performance is the best among the graphene-based FET DNA biosensor. We fabricate the R-GO FET biosensor by simply drop-casting the produced R-GO onto the sensor chip. Moreover, we demonstrate a new and robust method to immobilize PNA in the graphene-based FET biosensor. Specifically, we fabricate the FET biosensor chip with R-GO as the conducting material. Then we use PNA instead of DNA as the capture probe for targeting the complementary DNA sequence. Subsequently, the transfer curves of the biosensors are electrically measured before and after PNA–DNA hybridization. The hybridization event can be monitored according to the change of the electrical properties in the curves. Moreover, the high specificity of PNA–DNA hybridization is demonstrated by using the complementary, one-base mismatched, and non-complementary DNA sequences. Compared to the SiNW-based FET biosensor, the developed R-GO FET biosensor holds the following advantages: (i) simpler fabrication of a biosensor chip and easier processing, then higher yield and more cost-effective; (ii) more active detection area and surface roughness (theoretically 2630 m^2/g for single-layer graphene[38] *vs* 342 m^2/g for porous silicon nanowire[39]), leading to higher sensitivity potentially; (iii) greater carrier mobility (200 000 $cm^2/V\cdot s$ for graphene[40] *vs* 30–560 $cm^2/V\cdot s$ for silicon nanowire[41]), which means higher resolution and responsive speed in potential.

RESULTS AND DISCUSSION

The working principle of the R-GO FET biosensor for detection of DNA based on PNA–DNA hybridization is illustrated in Figure 1. First, the FET biosensor is fabricated on a SiO_2/Si substrate by the conventional macro-nano processing technologies. Second, the R-GO FET biosensor is obtained by drop-casting the R-GO onto the sensing channel as the conducting material. The R-GO suspensions were prepared using 98% hydrazine reported previously.[42] Subsequently, PASE (the linker molecule) is fixed on the R-GO surface though $\pi-\pi$ stacking interaction between the pyrene group and the graphene surface. Then, the PNA probe is immobilized through the covalently bond between the amino group on PNA and an amide bond on the other end of PASE, and ethanolamine solution is used to prevent possible nonspecific binding events. Finally, the target DNAs are applied onto the device for hybridization with probe PNA, and then a silver wire is used as the gate to realize a liquid-gated FET for electrical measurements. In principle, the hybridization of the complementary DNA with the probe PNA causes n-doping of the devices due to graphene–nucleotide non-electrostatic stacking interaction, as reported.[14,43,44] The PNA–DNA hybridization can be measured through monitoring the left shift of $I_{ds}-V_g$ curves of the devices. As a control, the introduction of the noncomplementary DNA to the PNA-functionalized devices does not result in a responsive signal.

Figure 2a shows the optical image of the FET biosensor chip. The chip is composed of six individual sensor arrays connected with the corresponding electrical lines and pads. Inset image shows the six pairs of electrodes, and the electrode separation channel width is 4 μm. The Raman spectrum of the R-GO is shown in Figure 2b. The Raman spectrum was conducted directly on a R-GO sheet on the SiO_2/Si substrate at room temperature. The spectrum displays the D band at 1350 cm^{-1} and the G band at 1600 cm^{-1}. The D/G intensity ratio is increased after reduction of GO, suggesting that there is a decrease in the average size of the sp^2 domains upon reduction of GO.[45] The result is consistent with that reported for chemically converted graphene,[45–47] indicating that the reduction of GO is successful as anticipated.

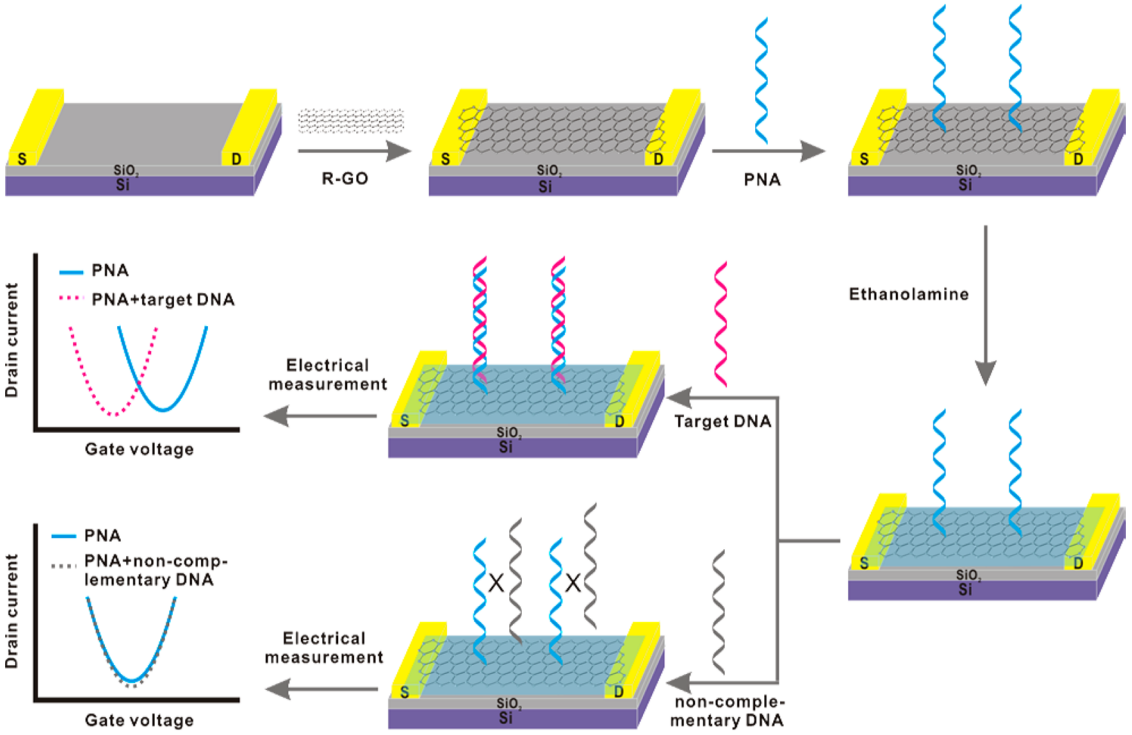

Figure 1. Schematic illustration of the R-GO FET biosensor for detection of DNA based on PNA−DNA hybridization.

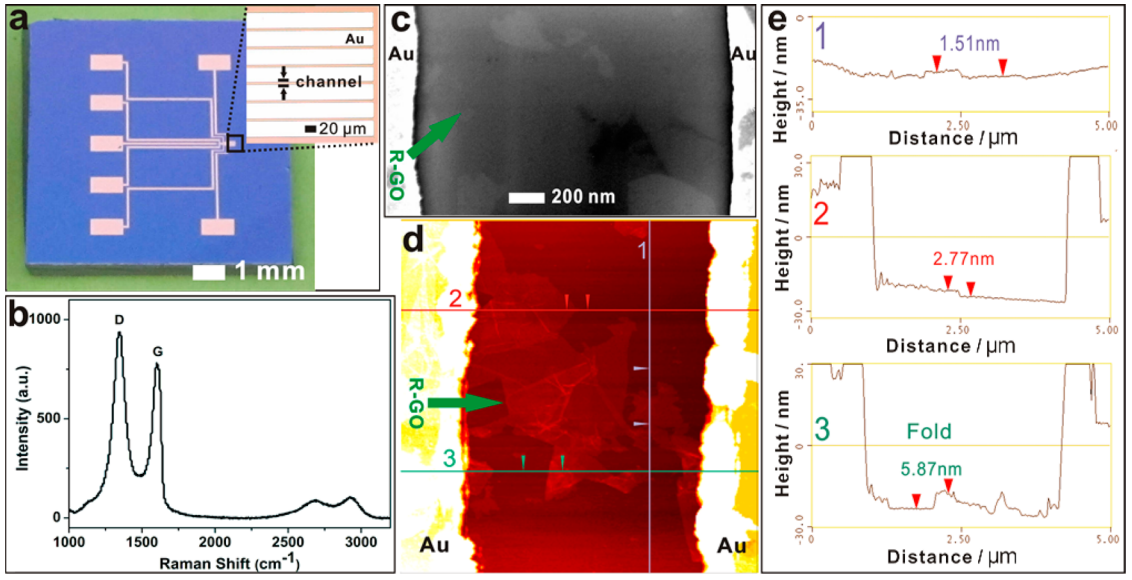

Figure 2. (a) Optical images of the R-GO FET biosensor chip. Six individual sensor arrays (inset). (b) Raman spectrum of the R-GO. (c) SEM image of a single R-GO sheet spanning across Au electrodes. (d) AFM image of the as-fabricated FET device, and lines 1, 2, and 3 represent the measuring line. (e) Height profiles from the three lines of the AFM image.

The scanning electron microscopy (SEM) image of the R-GO FET biosensor is illustrated in Figure 2c. It was seen that a few-layer R-GO sheet spanned across a pair of Au electrodes, and the darker color may be ascribed to the folds of the R-GO. The atomic force microscopy (AFM) image in Figure 2d shows more details about the structure of the R-GO inside the channel. It was clearly observed that the R-GO sheet connected a pair of Au electrodes and had wrinkles and folds. Figure 2e shows the three height profiles to demonstrate the thickness of the R-GO in the different regions. Based on the height profiles, the thickness of the R-GO sheet in lines 1, 2, and 3 is approximately 1.51, 2.77, and 5.87 nm, respectively. In line 1, the R-GO sheet was seen to be smooth. The thickness of the R-GO sheet might be ascribed to the wrinkle of the sheet in line 2. In line 3, we observed the fold of the R-GO sheet. So it is estimated that the thickness of the R-GO sheet

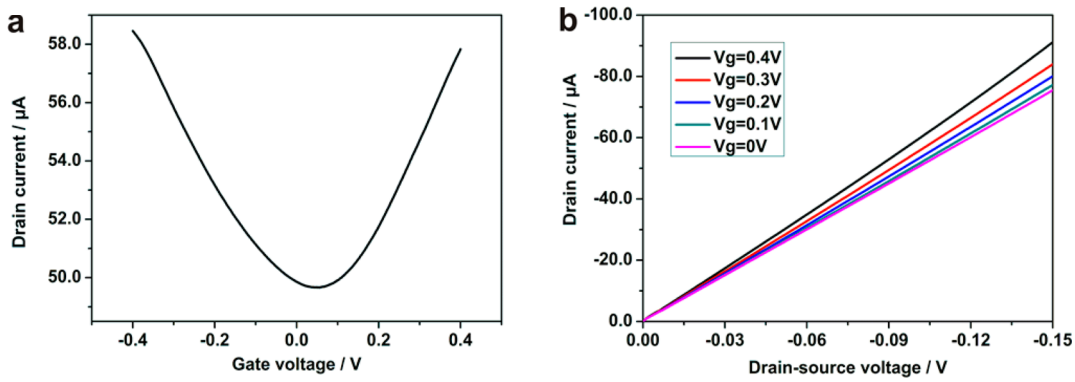

Figure 3. (a) $I_{ds}-V_g$ curve of the bare R-GO on a SiO_2/Si substrate (I_{ds} = 0.1 V). (b) $I_{ds}-V_{ds}$ output characteristics of the R-GO FET device. The gate voltage (V_g) is varied from 0 to 0.4 V with an interval of 0.1 V.

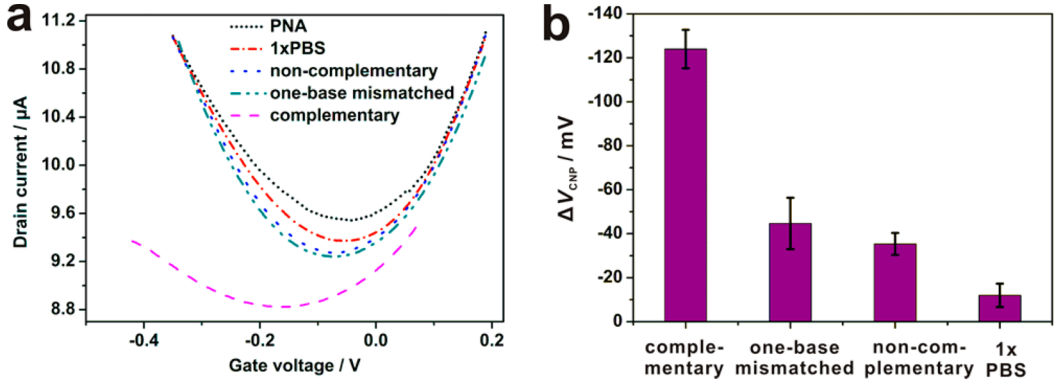

Figure 4. (a) Transfer characteristics and (b) shift of V_{CNP} of the PNA-immobilized R-GO FET biosensors incubated with 1× PBS, 1 nM noncomplementary DNA, 1 nM one-base mismatched DNA, and 1 nM complementary DNA.

assembled inside the channel is in the range of 1.5−6 nm. These results reveal that R-GO as the conducting material has been assembled to the channel surface between source and drain, and the R-GO FET biosensor has successfully been fabricated as expected.

To investigate the electrical properties of the R-GO FET device, the output and transfer characteristics of the R-GO FET biosensor were obtained prior to the functionalization of the R-GO. As shown in Figure 3, the typical $I_{ds}-V_g$ and $I_{ds}-V_{ds}$ curves were obtained. From the $I_{ds}-V_g$ curve in Figure 3a, the ambipolar characteristics could be clearly observed at a small range of gate voltage (from −0.4 to 0.4 V) under ambient conditions. The slight right shift of V_{CNP} (the gate voltage corresponding to the minimum conductance) suggests that the R-GO is p-doped by adsorbates in the environment.[48,49] The $I_{ds}-V_{ds}$ curve was obtained to further examine the electrical characteristics of the R-GO FET device in Figure 3b. The drain-source current decreases with a slight reduction of the gate voltage, indicating that the device response is sensitive to the gate voltage.[24]

To verify the specificity of the biosensor, noncomplementary DNA, one-base mismatched DNA, and complementary DNA were introduced to the PNA-functionalized R-GO FET devices. For the blank control test, the 1× PBS was conducted instead of the target DNA in the experiment. Figure 4a shows transfer characteristics of the PNA-immobilized R-GO FET biosensors incubated with 1× PBS, 1 nM noncomplementary DNA, 1 nM one-base mismatched DNA, and 1 nM complementary DNA. As illustrated, the shift of V_{CNP} for complementary DNA is much larger than that for 1× PBS, noncomplementary DNA, and one-base mismatched DNA. Figure 4b summarizes the shift of V_{CNP} of the biosensors incubated with 1× PBS, 1 nM noncomplementary DNA, 1 nM one-base mismatched DNA, and 1 nM complementary DNA. The ΔV_{CNP} (namely, the shift of V_{CNP} after incubated with 1× PBS or DNA relative to V_{CNP} of PNA) of 1× PBS, 1 nM noncomplementary DNA, 1 nM one-base mismatched DNA, and 1 nM complementary DNA are about −12, −35.3, −44.7, and −124 mV, respectively. The ΔV_{CNP} of noncomplementary DNA might be caused by a small amount of nonspecific adsorption. Due to one-base mismatch, the duplex between the one-base mismatched DNA and the probe PNA is unstable and may be unzipped during the washing steps, leading to a decreased response. The ΔV_{CNP} of one-base mismatched DNA was observed to be much smaller than that of complementary DNA, which is in good agreement with the previously reported results.[14] The data confirm that the biosensors can distinguish

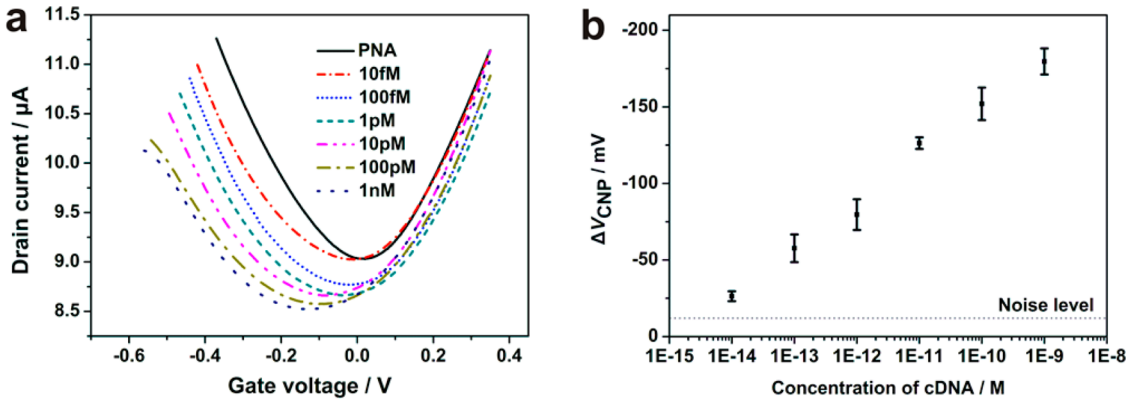

Figure 5. (a) Transfer characteristics and (b) shift of V_{CNP} of the PNA-immobilized R-GO FET biosensors hybridized with the complementary DNA at a series of concentrations (10 fM, 100 fM, 1 pM, 10 pM, 100 pM, and 1 nM). Dashed line represents the noise level (∼−12 mV) from the blank control test.

the complementary DNA from one-base mismatched DNA and noncomplementary DNA and can be used for SNP (single nucleotide polymorphism) detection. The results suggest that the R-GO FET biosensors are of high specificity.

The sensitivity of the R-GO FET biosensor was investigated by hybridization of various concentrations of complementary DNAs with the PNA-functionalized R-GO FET device, and the results are shown in Figure 5. From Figure 5a, we could see that the V_{CNP} of the devices shifted toward the left with increased concentration of the complementary DNA from 10 fM to 1 nM, and this result is in good agreement with that described by other reports.[14,27,43,50] Figure 5b shows the ΔV_{CNP} (namely, the shift of V_{CNP} after hybridizing with different concentration of complementary DNA relative to V_{CNP} of PNA) as a function of the concentration of the complementary DNA, which summarizes the left shift value of V_{CNP} at the corresponding concentrations of the complementary DNA. Dashed line in Figure 5b represents the noise level (∼−12 mV) from the blank control test. Then, the detection limit of 100 fM rather than 10 fM was achieved based on the signal that exceeds the background by 3-fold. Dong *et al.*[14] used CVD-grown graphene to fabricate liquid-gated transistors for DNA detection with detection sensitivity of 10 pM. Chen *et al.*[27] reported a FET biosensor based on CVD-grown graphene for label-free DNA detection with a detection limit of 1 pM (10^{-12} M). Yin *et al.*[50] fabricated Pt nanoparticle-decorated R-GO FET for real-time DNA detection with high sensitivity (2.4 nM). The performance comparison among various graphene-based FET DNA biosensors is listed in Table 1, which indicates that the R-GO FET biosensor reported in our research exhibits the highest sensitivity (100 fM) due to the PNA probe rather than DNA probe employed.

Finally, we investigated the reusability of the R-GO FET biosensors. To do so, PNA−DNA hybridization and dehybridization were run three times in sequence to examine the reusability of the devices. Dehybridization was conducted after PNA−DNA hybridization by immersing the biosensors into 8.3 M urea solution at room temperature for 5 min followed by rinsing with DI water.[51] Subsequently, rehybridization was performed with the same concentration of the complementary DNA on the same devices. After three cycles, the hybridization signal percentage of the second and the third hybridization was 96.67 and 83.33% of the first hybridization signal, respectively, which verifies that the R-GO FET biosensor has a reliable reusability and can be reused multiple times.

TABLE 1. Performance Comparison of Various Graphene-Based FET DNA Biosensors

	probe	sensitivity (fM)
Chen[27]	ssDNA	1000
Yin[50]	ssDNA	2400000
Dong[14]	ssDNA	10000
this work	PNA	100

CONCLUSIONS

In summary, we have constructed the FET biosensors based on chemically reduced graphene oxide for ultrasensitive label-free and highly specific detection of PNA−DNA hybridization. R-GO as the conducting material shows the obvious ambipolar characteristics at a small range of gate voltage on the liquid-gated FET devices under ambient conditions, and the devices are highly responsive to the low gate voltage. The PNA-modified R-GO FET biosensor exhibits greater sensitivity (100 fM) than the DNA-modified graphene FET biosensor because the PNA probe has a great sequence-specific affinity and stability to the target DNA. Furthermore, this PNA-functionalized biosensor can also discriminate complementary DNA from one-base mismatched DNA and noncomplementary DNA with high specificity. What is more, the R-GO FET biosensor shows a capability of reusability, which is

cost-effective in real application. Therefore, this biosensor with ultrasensitivity and high specificity provides a progressive way for potential applications in disease diagnostics.

MATERIALS AND METHODS

Materials. The PNA probe was synthesized by Bio-Synthesis, Inc. (Lewisville, Texas), and the DNAs purified by HPLC were purchased from Takara Biotechnology Co. Ltd. (Dalian, China). All PNAs and DNAs were 22-mer in length and diluted with 1× PBS. The sequence of the PNA probe is N-AACCACACAACCTAC-TACCTCA-C. The sequences of the DNAs employed for hybridization are 5′-TGAGGTAGTAGGTTGTGTGGTT-3′ (complementary), 5′-TGAGGTAGTAGGATGTGTGGTT-3′ (one-base mismatched), 5′-ATGCATGCATGCATGCATGCAA-3′ (noncomplementary). Graphite powder (99.99995%, 325 mesh) was purchased from Alfa Aesar Co., Ltd. (Tianjin, China). 1-Pyrenebutanoic acid succinimidyl ester (PASE) and ethanolamine were ordered from Sigma-Aldrich. $KMnO_4$, NaCl, 98% hydrazine, concentrated H_2SO_4, 35 wt % H_2O_2, and other chemicals were purchased from Generay Biotech Co. Ltd. (Shanghai, China). Ultrapure water was obtained from a Millipore water purification system (18.2 MΩ resistivity, Milli-Q Direct 8).

Preparation of R-GO. The R-GO suspensions were prepared using an aforementioned method.[42] First, graphite oxide (GO) was prepared by a modified Hummer's method.[52] Then, 15 mg of GO was added to 10 mL of 98% hydrazine followed by sonication for 10 min to produce a black suspension of hydrazinium graphene (HG), and the suspension was waved for 1 week for the purpose of thorough reduction of the GO and avoiding aggregation of the R-GO. The resulting R-GO suspensions could be stable for months with little aggregation.

Fabrication of R-GO FET Biosensors. The fabrication of the FET biosensor chip was completed by using the standard semiconductor technology. The gold electrodes were fabricated on SiO_2 (285 nm)/Si substrate to make source and drain electrodes using conventional macro-nano processing technologies including photolithography and electron-beam evaporation. The size of the whole device is 6 × 4.5 mm. The electrodes (50 nm thick) are 4 μm apart. To enhance the adhesion between the Au and the Si wafer, a 5 nm thick Ti layer was used. The diluted R-GO suspension was drop-casted onto the electrodes and thermally annealed at 150 °C in order to remove all solvent. After that, the R-GO biosensor chip was immersed in the Pirahna solution (7:3 v/v concd H_2SO_4/35% H_2O_2) and sonicated for 30 s to obtain few-layer R-GO, followed by thorough washing with DI water and drying with nitrogen.

Immobilization of PNA on the R-GO Surface. In order to immobilize PNA on the R-GO surface, a cross-linker molecule, PASE was used. The R-GO FET was treated with a 5 mM PASE in dimethylsulfoxide (DMSO) for 1 h at room temperature and washed with pure DMSO, ethanol, and DI water. The PASE-modified FET was then treated with 10 μM PNA for 2 h at room temperature followed by being rinsed in sequence with 1× PBS containing 0.2% SDS, 1× PBS, and DI water to remove the unreacted probe. The device was then incubated with 100 mM ethanolamine solution (pH 9.0) for 1 h to prevent possible nonspecific binding events and then rinsed by DI water.

Hybridization. PNA−DNA hybridization was conducted by dropping an appropriate concentration of complementary target DNA solution onto the device and incubated for 1 h. Then the chip was rinsed in sequence with 1× PBS containing 0.2% SDS, 1× PBS, and DI water to remove the unhybridized DNA sequence and dried with N_2. The same procedure was repeated by using the one-base mismatched and noncomplementary DNA sequences instead of the complementary target DNA sequence to perform the hybridization with the PNA probe.

Electrical Measurements. The liquid-gated R-GO FET devices were measured in a semiconductor parameter analyzer (Keithley 4200-SCS) coupled with a probe station (EverBeing BD-6). For $I_{ds}-V_g$ (I_{ds} is the drain-source current, V_g is the gate voltage) curve measurements of the R-GO devices, a silver wire was used as a gate electrode and a constant bias V_{ds} = 0.1 V (the drain-source voltage) was applied. $I_{ds}-V_{ds}$ curves were measured at an assigned V_g value.

Characterizations. Raman spectrum was obtained using a DXR confocal Raman microscopy system (Thermo Scientific, America) with a 532 nm HeNe laser system. A Zeiss UltraPlus FE-SEM was used for SEM characterization of the device at a 5 kV acceleration voltage. AFM was conducted with a DI Nanoscope IV AFM with a cantilever (VEECO RTESP).

Conflict of Interest: The authors declare no competing financial interest.

Acknowledgment. This work was supported by the National Natural Science Foundation of China (Nos. 21275040, 61322105, and 61172001) and the Natural Science Foundation of Hubei Province (No. 2013CFA061).

REFERENCES AND NOTES

1. Bowtell, D. D. Options Available—from Start to Finish—for Obtaining Expression Data by Microarray. *Nat. Genet.* **1999**, *21*, 25–32.
2. Janasek, D.; Franzke, J.; Manz, A. Scaling and the Design of Miniaturized Chemical-Analysis Systems. *Nature* **2006**, *442*, 374–380.
3. Drummond, T. G.; Hill, M. G.; Barton, J. K. Electrochemical DNA Sensors. *Nat. Biotechnol.* **2003**, *21*, 1192–1199.
4. Hay Burgess, D. C.; Wasserman, J.; Dahl, C. A. Global Health Diagnostics. *Nature* **2006**, *444*, 1–2.
5. Du, Y.; Guo, S.; Dong, S.; Wang, E. An Integrated Sensing System for Detection of DNA Using New Parallel-Motif DNA Triplex System and Graphene−Mesoporous Silica−Gold Nanoparticle Hybrids. *Biomaterials* **2011**, *32*, 8584–8592.
6. Panke, O.; Kirbs, A.; Lisdat, F. Voltammetric Detection of Single Base-Pair Mismatches and Quantification of Label-Free Target ssDNA Using a Competitive Binding Assay. *Biosens. Bioelectron.* **2007**, *22*, 2656–2662.
7. Guo, S.; Du, D.; Tang, L.; Ning, Y.; Yao, Q.; Zhang, G. J. PNA-Assembled Graphene Oxide for Sensitive and Selective Detection of DNA. *Analyst* **2013**, *138*, 3216–3220.
8. Liu, B.; Sun, Z.; Zhang, X.; Liu, J. Mechanisms of DNA Sensing on Graphene Oxide. *Anal. Chem.* **2013**, *85*, 7987–7993.
9. Lu, C. H.; Yang, H. H.; Zhu, C. L.; Chen, X.; Chen, G. N. A Graphene Platform for Sensing Biomolecules. *Angew. Chem.* **2009**, *48*, 4785–4787.
10. Wang, Z.; Zhang, J.; Yin, Z.; Wu, S.; Mandler, D.; Zhang, H. Fabrication of Nanoelectrode Ensembles by Electrodeposiston of Au Nanoparticles on Single-Layer Graphene Oxide Sheets. *Nanoscale* **2012**, *4*, 2728–2733.
11. Du, D.; Guo, S.; Tang, L.; Ning, Y.; Yao, Q.; Zhang, G.-J. Graphene-Modified Electrode for DNA Detection *via* PNA−DNA Hybridization. *Sens. Actuators, B* **2013**, *186*, 563–570.
12. Zhang, G. J.; Zhang, G.; Chua, J. H.; Chee, R. E.; Wong, E. H.; Agarwal, A.; Buddharaju, K. D.; Singh, N.; Gao, Z.; Balasubramanian, N. DNA Sensing by Silicon Nanowire: Charge Layer Distance Dependence. *Nano Lett.* **2008**, *8*, 1066–1070.
13. Dong, X.; Lau, C. M.; Lohani, A.; Mhaisalkar, S. G.; Kasim, J.; Shen, Z.; Ho, X.; Rogers, J. A.; Li, L.-J. Electrical Detection of Femtomolar DNA *via* Gold-Nanoparticle Enhancement in Carbon-Nanotube-Network Field-Effect Transistors. *Adv. Mater.* **2008**, *20*, 2389–2393.
14. Dong, X.; Shi, Y.; Huang, W.; Chen, P.; Li, L. J. Electrical Detection of DNA Hybridization with Single-Base Specificity Using Transistors Based on CVD-Grown Graphene Sheets. *Adv. Mater.* **2010**, *22*, 1649–1653.

15. Star, A.; Tu, E.; Niemann, J.; Gabriel, J. C.; Joiner, C. S.; Valcke, C. Label-Free Detection of DNA Hybridization Using Carbon Nanotube Network Field-Effect Transistors. *Proc. Natl. Acad. Sci. U.S.A.* **2006**, *103*, 921–926.
16. Zhang, G. J.; Ning, Y. Silicon Nanowire Biosensor and Its Applications in Disease Diagnostics: A Review. *Anal. Chim. Acta* **2012**, *749*, 1–15.
17. Zhang, G. J.; Huang, M. J.; Ang, J. J.; Yao, Q.; Ning, Y. Label-Free Detection of Carbohydrate−Protein Interactions Using Nanoscale Field-Effect Transistor Biosensors. *Anal. Chem.* **2013**, *85*, 4392–4397.
18. Chua, J. H.; Chee, R. E.; Agarwal, A.; Wong, S. M.; Zhang, G. J. Label-Free Electrical Detection of Cardiac Biomarker with Complementary Metal-Oxide Semiconductor-Compatible Silicon Nanowire Sensor Arrays. *Anal. Chem.* **2009**, *81*, 6266–6271.
19. Zhang, G. J.; Huang, M. J.; Luo, Z. H.; Tay, G. K.; Lim, E. J.; Liu, E. T.; Thomsen, J. S. Highly Sensitive and Reversible Silicon Nanowire Biosensor To Study Nuclear Hormone Receptor Protein and Response Element DNA Interactions. *Biosens. Bioelectron.* **2010**, *26*, 365–370.
20. Bradley, K.; Briman, M.; Star, A.; Gruner, G. Charge Transfer from Adsorbed Proteins. *Nano Lett.* **2004**, *4*, 253–256.
21. Besteman, K.; Lee, J. O.; Wiertz, F. G. M.; Heering, H. A.; Dekker, C. Enzyme-Coated Carbon Nanotubes as Single-Molecule Biosensors. *Nano Lett.* **2003**, *3*, 727–730.
22. Huang, Y.; Dong, X.; Shi, Y.; Li, C. M.; Li, L. J.; Chen, P. Nanoelectronic Biosensors Based on CVD Grown Graphene. *Nanoscale* **2010**, *2*, 1485–1488.
23. Lin, Y. M.; Avouris, P. Strong Suppression of Electrical Noise in Bilayer Graphene Nanodevices. *Nano Lett.* **2008**, *8*, 2119–2125.
24. Chang, J.; Mao, S.; Zhang, Y.; Cui, S.; Zhou, G.; Wu, X.; Yang, C. H.; Chen, J. Ultrasonic-Assisted Self-Assembly of Monolayer Graphene Oxide for Rapid Detection of *Escherichia coli* Bacteria. *Nanoscale* **2013**, *5*, 3620–3626.
25. Kim, D. J.; Sohn, I. Y.; Jung, J. H.; Yoon, O. J.; Lee, N. E.; Park, J. S. Reduced Graphene Oxide Field-Effect Transistor for Label-Free Femtomolar Protein Detection. *Biosens. Bioelectron.* **2013**, *41*, 621–626.
26. Ohno, Y.; Maehashi, K.; Yamashiro, Y.; Matsumoto, K. Electrolyte-Gated Graphene Field-Effect Transistors for Detecting pH and Protein Adsorption. *Nano Lett.* **2009**, *9*, 3318–3322.
27. Chen, T. Y.; Loan, P. T.; Hsu, C. L.; Lee, Y. H.; Tse-Wei Wang, J.; Wei, K. H.; Lin, C. T.; Li, L. J. Label-Free Detection of DNA Hybridization Using Transistors Based on CVD Grown Graphene. *Biosens. Bioelectron.* **2013**, *41*, 103–109.
28. Novoselov, K. S.; Geim, A. K.; Morozov, S. V.; Jiang, D.; Zhang, Y.; Dubonos, S. V.; Grigorieva, I. V.; Firsov, A. A. Electric Field Effect in Atomically Thin Carbon Films. *Science* **2004**, *306*, 666–669.
29. Ohno, Y.; Maehashi, K.; Matsumoto, K. Chemical and Biological Sensing Applications Based on Graphene Field-Effect Transistors. *Biosens. Bioelectron.* **2010**, *26*, 1727–1730.
30. Li, X.; Cai, W.; An, J.; Kim, S.; Nah, J.; Yang, D.; Piner, R.; Velamakanni, A.; Jung, I.; Tutuc, E.; *et al.* Large-Area Synthesis of High-Quality and Uniform Graphene Films on Copper Foils. *Science* **2009**, *324*, 1312–1314.
31. Reina, A.; Jia, X.; Ho, J.; Nezich, D.; Son, H.; Bulovic, V.; Dresselhaus, M. S.; Kong, J. Large Area, Few-Layer Graphene Films on Arbitrary Substrates by Chemical Vapor Deposition. *Nano Lett.* **2009**, *9*, 30–35.
32. Park, S.; An, J.; Jung, I.; Piner, R. D.; An, S. J.; Li, X.; Velamakanni, A.; Ruoff, R. S. Colloidal Suspensions of Highly Reduced Graphene Oxide in a Wide Variety of Organic Solvents. *Nano Lett.* **2009**, *9*, 1593–1597.
33. Li, D.; Muller, M. B.; Gilje, S.; Kaner, R. B.; Wallace, G. G. Processable Aqueous Dispersions of Graphene Nanosheets. *Nat. Nanotechnol.* **2008**, *3*, 101–105.
34. Nielsen, P. E.; Egholm, M.; Berg, R. H.; Buchardt, O. Sequence-Selective Recognition of DNA by Strand Displacement with a Thymine-Substituted Polyamide. *Science* **1991**, *254*, 1497–1500.
35. Nielsen, P. E.; Egholm, M.; Buchardt, O. Peptide Nucleic Acid (PNA). A DNA Mimic with a Peptide Backbone. *Bioconjugate Chem.* **1994**, *5*, 3–7.
36. Zhang, G. J.; Chua, J. H.; Chee, R. E.; Agarwal, A.; Wong, S. M.; Buddharaju, K. D.; Balasubramanian, N. Highly Sensitive Measurements of PNA−DNA Hybridization Using Oxide-Etched Silicon Nanowire Biosensors. *Biosens. Bioelectron.* **2008**, *23*, 1701–1707.
37. Hyrup, B.; Egholm, M.; Nielsen, P. E.; Wittung, P.; Norden, B.; Buchardt, O. Structure−Activity Studies of the Binding of Modified Peptide Nucleic Acids (PNAs) to DNA. *J. Am. Chem. Soc.* **1994**, *116*, 7964–7970.
38. McAllister, M. J.; Li, J.-L.; Adamson, D. H.; Schniepp, H. C.; Abdala, A. A.; Liu, J.; Herrera-Alonso, M.; Milius, D. L.; Car, R.; Prud'homme, R. K.; *et al.* Single Sheet Functionalized Graphene by Oxidation and Thermal Expansion of Graphite. *Chem. Mater.* **2007**, *19*, 4396–4404.
39. Hochbaum, A. I.; Gargas, D.; Hwang, Y. J.; Yang, P. Single Crystalline Mesoporous Silicon Nanowires. *Nano Lett.* **2009**, *9*, 3550–3554.
40. Morozov, S. V.; Novoselov, K. S.; Katsnelson, M. I.; Schedin, F.; Elias, D. C.; Jaszczak, J. A.; Geim, A. K. Giant Intrinsic Carrier Mobilities in Graphene and Its Bilayer. *Phys. Rev. Lett.* **2008**, *100*, 016602.
41. Cui, Y.; Zhong, Z.; Wang, D.; Wang, W. U.; Lieber, C. M. High Performance Silicon Nanowire Field Effect Transistors. *Nano Lett.* **2003**, *3*, 149–152.
42. Tung, V. C.; Allen, M. J.; Yang, Y.; Kaner, R. B. High-Throughput Solution Processing of Large-Scale Graphene. *Nat. Nanotechnol.* **2009**, *4*, 25–29.
43. Lin, C.-T.; Loan, P. T. K.; Chen, T.-Y.; Liu, K.-K.; Chen, C.-H.; Wei, K.-H.; Li, L.-J. Label-Free Electrical Detection of DNA Hybridization on Graphene Using Hall Effect Measurements: Revisiting the Sensing Mechanism. *Adv. Funct. Mater.* **2013**, *23*, 2301–2307.
44. Manohar, S.; Mantz, A. R.; Bancroft, K. E.; Hui, C. Y.; Jagota, A.; Vezenov, D. V. Peeling Single-Stranded DNA from Graphite Surface To Determine Oligonucleotide Binding Energy by Force Spectroscopy. *Nano Lett.* **2008**, *8*, 4365–4372.
45. Stankovich, S.; Dikin, D. A.; Piner, R. D.; Kohlhaas, K. A.; Kleinhammes, A.; Jia, Y.; Wu, Y.; Nguyen, S. T.; Ruoff, R. S. Synthesis of Graphene-Based Nanosheets *via* Chemical Reduction of Exfoliated Graphite Oxide. *Carbon* **2007**, *45*, 1558–1565.
46. Fowler, J. D.; Allen, M. J.; Tung, V. C.; Yang, Y.; Kaner, R. B.; Weiller, B. H. Practical Chemical Sensors from Chemically Derived Graphene. *ACS Nano* **2009**, *3*, 301–306.
47. Guo, H. L.; Wang, X. F.; Qian, Q. Y.; Wang, F. B.; Xia, X. H. A Green Approach to the Synthesis of Graphene Nanosheets. *ACS Nano* **2009**, *3*, 2653–2659.
48. Jung, I.; Dikin, D. A.; Piner, R. D.; Ruoff, R. S. Tunable Electrical Conductivity of Individual Graphene Oxide Sheets Reduced at "Low" Temperatures. *Nano Lett.* **2008**, *8*, 4283–4287.
49. Wang, X.; Li, X.; Zhang, L.; Yoon, Y.; Weber, P. K.; Wang, H.; Guo, J.; Dai, H. n-Doping of Graphene through Electrothermal Reactions with Ammonia. *Science* **2009**, *324*, 768–771.
50. Yin, Z.; He, Q.; Huang, X.; Zhang, J.; Wu, S.; Chen, P.; Lu, G.; Chen, P.; Zhang, Q.; Yan, Q.; *et al.* Real-Time DNA Detection Using Pt Nanoparticle-Decorated Reduced Graphene Oxide Field-Effect Transistors. *Nanoscale* **2012**, *4*, 293–297.
51. Zhang, G. J.; Luo, Z. H.; Huang, M. J.; Tay, G. K.; Lim, E. J. Morpholino-Functionalized Silicon Nanowire Biosensor for Sequence-Specific Label-Free Detection of DNA. *Biosens. Bioelectron.* **2010**, *25*, 2447–2453.
52. Kovtyukhova, N. I.; Ollivier, P. J.; Martin, B. R.; Mallouk, T. E.; Chizhik, S. A.; Buzaneva, E. V.; Gorchinskiy, A. D. Layer-by-Layer Assembly of Ultrathin Composite Films from Micron-Sized Graphite Oxide Sheets and Polycations. *Chem. Mater.* **1999**, *11*, 771–778.